

## LPS에 의해 자극된 RAW264.7 세포에 대한 계지가출부탕의 항염증활동

정민정<sup>1</sup> · 이승연<sup>2</sup> · 유선애<sup>2</sup> · 강경화<sup>3</sup>

<sup>1</sup>우석대학교 한의과대학 한방소아과학교실

<sup>2</sup>동의대학교 한의과대학 한방소아과학교실

<sup>3</sup>동의대학교 한의과대학 생리학교실

### Abstract

#### Anti-inflammatory Activities of GyejigaChulBuTang on Lipopolysaccharide-stimulated RAW264.7 Cells

Min-Jeong Jeong<sup>1</sup> · Seung-Yeon Lee<sup>2</sup> · Sun-Ae Yu<sup>2</sup> · Kyung-Hwa Kang<sup>3</sup>

<sup>1</sup> Department of Korean Pediatrics, College of Korean Medicine, Woosuk University

<sup>2</sup> Department of Korean Pediatrics, College of Korean Medicine, Dongeui University

<sup>3</sup> Department of Physiology, College of Korean Medicine, Dongeui University

#### Objectives

GyejigaChulBuTang (GCBT) is a prescription used to treat acute and chronic arthritis in Korea, China, and Japan. This study assessed the anti-inflammatory and anti-oxidant activities of GCBT on lipopolysaccharide (LPS)-stimulated RAW264.7 macrophage cells.

#### Methods

Raw264.7 cells were pretreated with or without GCBT for 1 hour prior to incubation with LPS. Anti-inflammatory activity of GCBT was evaluated with reference to gene expression and production levels of proinflammatory cytokines (TNF $\alpha$ , IL-1 $\beta$ , IL-6, GM-CSF and INF $\gamma$ ) and inflammatory mediators (iNOS, COX-2, NO and PGE $_2$ ). In addition, intracellular ROS generation and signal transduction of MAPK family, PI3K/Akt and I $\kappa$ B $\alpha$ /NF $\kappa$ B was investigated.

#### Results

Prior treatment with GCBT inhibited elevation of TNF $\alpha$ , IL-1 $\beta$ , IL-6, GM-CSF, INF $\gamma$ , NO and PGE $_2$ , together with their cognate mRNAs in a dose-dependent manner. Intracellular ROS contents were similarly reduced. These effects were due to inhibition of LPS-induced phosphorylation of MAPK family, PI3K/Akt and I $\kappa$ B $\alpha$  as well as nuclear translocation of NF $\kappa$ B.

#### Conclusions

GCBT suppresses pro-inflammatory mediators. GCBT has potential in the treatment of juvenile rheumatoid arthritis associated with inflammation.

**Key words** : GyejigaChulBuTang, RAW264.7 cells, Proinflammatory cytokine, Juvenile rheumatoid arthritis, Inflammation

Received: July 25, 2014 • Revised: August 8, 2014 • Accepted: August 10, 2014

Corresponding Author: Kyung-Hwa Kang

Department of Physiology, College of Korean Medicine, Dongeui University  
52-57, Yangjeong-ro, Busanjin-gu, Busan, 614-851, Republic of Korea.

Tel: +82-51-850-7423 / Fax: +82-51-853-4036

E-mail: ghkang@deu.ac.kr

© The Association of Pediatrics of Korean Medicine. All rights reserved. This is an open-access article distributed under the terms of the Creative Commons Attribution Non-Commercial License (<http://creativecommons.org/licenses/by-nc/3.0/>), which permits unrestricted non-commercial use, distribution, and reproduction in any medium, provided the original work is properly cited.

## I. Introduction

Juvenile rheumatoid arthritis (JRA) is the most common arthritic autoimmune disease of childhood. The disease appears prior to 16 years of age and persists for more than 6 weeks<sup>1</sup>. Similar to other autoimmune diseases, the etiology of JRA remains unknown, although JRA is influenced by complex genetic and perhaps environmental factors<sup>2-4</sup>. JRA has been classified as oligoarthritis, polyarthritis and systemic arthritis based on symptoms that within 6 months after the onset of disease<sup>5</sup>. Although JRA is heterogeneous in character, overproduced proinflammatory cytokines including tumor necrosis factor-alpha (TNF $\alpha$ ), interleukin (IL)-1 $\beta$  and IL-6 are key regulators in the pathogenic process<sup>6-10</sup>. The interactions among activated macrophages, T cells, B cells and non-hematopoietic cells including fibroblasts produce proinflammatory cytokines and induce a chronic inflammation in the pathogenesis of JRA. The inflammatory process may lead to progressive synovitis, pannus formation, cartilage destruction and bone erosion, which causes loss of function and disability<sup>11</sup>. In Korean Medicine, JRA has been recognized as belonging to the categories of 'impediment symptom (痺證)' and 'joint-running wind (歷節風)', along with adult rheumatoid arthritis<sup>12,13</sup>.

Gyejigachulbutang (GCBT, 桂枝加朮附湯) has long been used to treat acute and chronic inflammatory diseases involving rheumatoid arthritis in traditional Korean medicine. However, its underlying mechanism of anti-inflammation has not been clearly defined. Presently, we investigated whether GCBT inhibits proinflammatory cytokines, other inflammatory mediators, and signal transduction on lipopolysaccharide (LPS)-stimulated RAW 264.7 murine macrophage cells to identify the anti-inflammatory effects of GCBT.

## II. Materials and Methods

### 1. Preparation of GCBT

GCBT was prepared by mixing seven herbal medicines, 60 g Cinnamomi Cortex Spissus (*Cinnamomum cassia* Blume, Lot. No. M-L01), 60 g Paeoniae Radix Rubra (*Paeonia obovata* Max., Lot. No. MR-L02), 60 g Zingiberis Rhizoma Crudus (*Zingiber officinale* Roscoe, Lot. No. D-K01), 60 g Zizyphi Fructus (*Zizyphus jujuba* Miller var., Lot. No. D-K02), 60 g Atractylodis Rhizoma (*Atractylodes chinensis* Koidzumi, Lot. No. M-L02), 40 g Glycyrrhizae Radix et Rhizoma (*Glycyrrhiza uralensis* Fischer, Lot. No. M-L02), and 40 g Pulvis Aconiti Tuberis Purificatum (*Aconitium carmichaeli* Debeaux, Lot. No. M-L01), obtained from Sae-rom Pharmaceutical (Anseong, Gyeonggi-do, Korea). The herbal formula GCBT (380 g) was extracted for 3 hrs by boiling with distilled water (Table 1). The extract was filtered and evaporated on a rotary evaporator under a reduced pressure. The extract was lyophilized and the yield of the extract was approximately 10.8%. A voucher specimen (G20110322) was deposited at Oriental Physiology Laboratory, Dongguk University. The extract power was stored at -20 °C until use.

### 2. Materials

Dulbecco's modified Eagle's medium (DMEM), fetal bovine serum (FBS), penicillin and streptomycin were obtained from Gibco (Grand Island, NY, USA). MTT (3-[4,5-dimethylthiazol-2-yl]-2,5-diphenyltetrazolium bromide), and LPS from *Escherichia coli* 0111:B4 were purchased from Sigma-Aldrich (St. Louis, MO, USA). 5-(6)-Chloromethyl-2', 7'-dichlorodihydrofluorescein diacetate

Table 1. Composition of GCBT used in this study.

Herbal Names	Scientific Names	Weight (g)
肉桂	<i>Cinnamomum cassia</i> PRESL	6
芍藥	<i>Paeonia lactiflora</i> PALL	6
生薑	<i>Zingiber officinale</i> ROSC	6
大棗	<i>Zizyphus jujuba</i>	6
蒼朮	<i>Atractylodes japonica</i>	6
甘草	<i>Glycyrrhiza uralensis</i>	4
炮附子	<i>Processed Aconitium carmichaeli</i>	4
Total		38

(CM-H<sub>2</sub>DCFDA) was purchased from Molecular Probes (Eugene, OR, USA). Enzyme-linked immunosorbent assay (ELISA) kits for determining prostaglandin E<sub>2</sub> (PGE<sub>2</sub>) and cytokines were purchased from Cayman Chemical (Ann Arbor, MI, USA) and BD Biosciences Pharmingen (San Diego, CA, USA). Antibody against inducible nitric oxide synthase (iNOS) and cyclooxygenase-2 (COX-2) was obtained from BD Biosciences Pharmingen. Phospho-specific or total antibodies to mitogen-activated protein kinase (MAPK) family members extracellular signal-regulated kinase (ERK), c-jun, N-terminal kinase (JNK, and p38; phosphoinositol-3-kinase (PI3K), Akt, IκBα, transcription factors [nuclear factor-kappa B (NFκB) and p65], and β-actin were obtained from Cell Signaling Technologies (Beverly, MA, USA). All other reagents were of the highest grade commercially available.

### 3. Cell line and culture condition

RAW264.7 murine macrophage cells obtained from American Type Culture Collection (Manassas, VA, USA) and cultured in DMEM with 10% FBS, penicillin, and streptomycin and incubated at 37 °C under humidified conditions in an atmosphere containing 5% CO<sub>2</sub>.

### 4. Measurement of cell viability

Cell viability was estimated by the MTT assay. RAW264.7 cells were incubated into 24-well plate (5 × 10<sup>4</sup> cells/mL) and cultured overnight. After incubation, the culture medium was replaced with complete growth medium and the cells were either left untreated or treated with GCBT (1, 2.5, 5, 7.5, and 10 mg/mL) for 1 h at 37 °C in 5% CO<sub>2</sub>. MTT (5 mg/mL) was added to each well and the plates were incubated at 37 °C in the dark for 4 h. The supernatant of each well was vacuum-aspirated and 200 μl of dimethylsulfoxide (DMSO) was added to each well. The plates were agitated to enhance the dissolution of the formazan that formed. Cell viability was determined using a Spectra Max M2 microplate reader (Molecular Devices, Sunnyvale, CA, USA) at 570 nm.

### 5. Measurement of proinflammatory cytokines produced by RAW264.7 cells

RAW264.7 cells (5 × 10<sup>5</sup> cells/mL) were seeded into 24-well plates. Cells were left untreated or pretreated with GCBT (2, 4, and 8 mg/mL) for 1 h and then stimulated with 1 μg/mL of LPS for an additional 3 hrs at 37 °C and 5% CO<sub>2</sub>. To stop reaction, the plate was put on ice for 10 min and the supernatants were transferred to individual e-tubes. Supernatants were centrifuged at 5,000 rpm for 10 min and transferred to new e-tubes. The level of cytokine concentration was determined by ELISA according to the manufacturer's instructions.

### 6. Measurement of PGE<sub>2</sub> release by RAW264.7 cells

RAW264.7 cells (5 × 10<sup>5</sup> cells/mL) were seeded into 96-well plates. Cells were untreated or pretreated with GCBT (2, 4, and 8 mg/mL) for 1 h and then stimulated with 1 μg/mL of LPS for an additional 4 hrs at 37 °C and 5% CO<sub>2</sub>. The level of PGE<sub>2</sub> production from endogenous arachidonic acid metabolism was measured in cell culture supernatants of the RAW264.7 cells by ELISA according to the manufacturer's instructions.

### 7. Nitrite assay

RAW264.7 cells (5 × 10<sup>5</sup> cells/mL) were seeded into 24-well plates. Cells were untreated or pretreated with GCBT (2, 4, and 8 mg/mL) for 1 h and then stimulated with 1 μg/mL of LPS for an additional 24 hrs at 37 °C and 5% CO<sub>2</sub>. Nitrite accumulation in culture was measured colorimetrically by the Griess reaction using Griess reagent (Sigma, St Louis, MO, USA). For the assay, equal volumes of cultured medium and Griess reagent were mixed and the absorption coefficient was calibrated using a sodium nitrite solution standard (Sigma, St Louis, MO, USA). The absorbance of each sample after Griess reaction was determined by the aforementioned Spectra Max M2 microplate reader at 540 nm.

### 8. Measurement of intracellular ROS level

RAW264.7 cells (2.5 × 10<sup>5</sup> cells/mL) were seeded into 96-well plates. Cells were washed twice with phosphate buffered saline (PBS) and incubated with 10 μM of CM-H<sub>2</sub>DCFDA for 30 min. The treated cells were washed

with PBS and incubated with or without GCBT (2, 4, and 8 mg/mL) for 30 min. GCBT treated cells were stimulated by 1 µg/mL of LPS and incubated for an additional 1 h at 37 °C and 5% CO<sub>2</sub>. After incubation, the supernatants were measured with an excitation wavelength of 490 nm and an emission wavelength of 530 nm with the aforementioned Spectra Max M2 fluorometer. The percent DCF oxidation from RAW264.7 cells by the test sample was calculated using the following equation:

$$\text{DCF oxidation (\%)} = (\text{T}-\text{C}) / \text{C} \times 100,$$

where C is the control and T is the test sample.

## 9. RT-PCR

RAW264.7 cells were untreated or pretreated with GCBT (2, 4, and 8 mg/mL) for 1 h, and then stimulated with 1 µg/mL of LPS for an additional 3 hrs. Thereafter, cells were washed twice with ice-cold PBS and then total RNA was extracted from the cells using TRIzol reagent (Invitrogen, Carlsbad, CA, USA) according to the manufacturer's instructions. The following primers were used to amplify IL-1β, IL-6, TNF-α, granulocyte-macrophage colony-stimulating factor (GM-CSF), interferon-gamma (INF-γ), iNOS, COX-2, and 18S: for IL-1β, 5'-AAG CTC TCC ACC TCA ATG GAC A-3' (sense), 5'-GTC TGC TCA TTC ACG AAA ABB GAG-3' (anti-sense); for IL-6, 5'-TCC AGT TGC CTT CTT GGG AC-3' (sense), 5'-GTG TAA TTA AGC CTC CGA CTT G-3' (anti-sense); for TNF-α, 5'-GCG ACG TGG AAC TGG CAG AAG -3' (sense), 5'-TCC ATG CCG TTG GTT AGG AGG-3' (anti-sense); for GM-CSF, 5'-AGC CTT AAA ACC TTT CTG ACT GAT A-3' (sense), 5'-TCC AAG CTG AGT CAG CGT TTT CAG A-3' (anti-sense); for INF-γ, 5'-TCA AGT GGC ATA GAT GTC GAA GAA-3' (sense), 5'-TGG CTC TGC AGG ATT TTC ATG-3' (anti-sense); for iNOS 5'-CTG CAG CAC TTG GAT CAG GAA CCT G-3' (sense), 5'-GGG AGT AGC CTG TGT GCA CCT GGA A-3' (anti-sense); for COX-2, 5'-TTG AAG ACC AGG AGT ACC GC-3' (sense), 5'-GGT ACA GT CCC ATG ACA TCG-3' (anti-sense); for 18S, 5'-GTA ACC CGT TGA ACC CCA TT-3' (sense), 5'-CCA TCC AAT CGG TAG TAG CG -3' (anti-sense). PCR reaction was performed with a GeneAmp PCR System 9700 (Applied

Biosystems, Foster City, CA, USA). PCR products were electrophoresed in 2% (w/v) agarose gels and stained with ethidium bromide. The value of each mRNA was normalized to the amount of 18S, which was utilized as a housekeeping gene for each experimental condition. Bands were quantified using Scion Image beta 3b densitometry software (Scion, Frederick, MD, USA).

## 10. Western blot analysis

RAW264.7 cells were untreated or pretreated with GCBT (2, 4, and 8 mg/mL) for 1 h and then stimulated with 1 µg/mL of LPS for an additional 5 min (for p-ERK, p-JNK, p-p38, p-PI3K, and p-Akt), 1 h (for p-IκBα, IκBα and NFκB), or 24 hrs (for iNOS and COX-2) at 37 °C and 5% CO<sub>2</sub>. Total cell extracts were lysed with an ice-cold lysis buffer consisting of 10 mM Tris-HCl (pH 7.4), 5 mM NaF, 1 mM Na<sub>3</sub>VO<sub>4</sub>, 1 mM ethylenediaminetetraacetic acid (EDTA), and 1 mM ethylene glycol bis (2-aminoethyl ether) tetraacetic acid (EGTA). To investigate the degradation of IκBα and nuclear translocation of NFκB p65, cytoplasmic and nuclear extracts were prepared. Cytosolic extracts were prepared in low-salt buffer consisting of 20 mM N-(2-hydroxyethyl) piperazine-N-2-ethanesulfonic acid (HEPES; pH 7.9), 10 mM KCl, 0.1 mM Na<sub>3</sub>VO<sub>4</sub>, 1 mM EDTA, 1 mM EGTA, 0.2% Igepal CA-630, 10% glycerol, 0.5 mM phenylmethylsulfonyl fluoride (PMSF), and 1 mM dithiothreitol (DTT). Nuclear extracts were prepared in high-salt buffer consisting of 20 mM HEPES (pH 7.9), 400 mM NaCl, 10 mM KCl, 0.1 mM Na<sub>3</sub>VO<sub>4</sub>, 1 mM EDTA, 1 mM EGTA, 20% glycerol, 0.5 mM PMSF, and 1 mM DTT. Proteins in total cell extracts (for p-ERK, p-JNK, p-p38, p-PI3K, p-Akt, iNOS and COX-2), cytoplasmic extracts (for p-IκBα and IκBα), and nuclear extracts (for NFκB p65) were separated with 10% sodium dodecyl sulfate-polyacrylamide gel electrophoresis (SDS-PAGE) and transferred to nitrocellulose transfer membranes (Whatman GmbH, Dassel, Germany). The membranes were blocked with 5% skim milk in 10 mM Tris-HCl, pH 7.5, 150 mmol/L NaCl, and 0.05% Tween 20 (TBST) for 1 h, washed, and then incubated with primary antibody (diluted 1/1000 in 5% skim milk in TBST) overnight at 4 °C. The membranes were then incubated for 1 h with horseradish perox-

idase-conjugated anti-mouse IgG or anti-rabbit IgG antibody (diluted 1/2000 in 5% skim milk in TBST) and immunoreactive bands were developed using an enhanced chemiluminescence reagents (ECL; Amersham, Little Chalfont, UK).  $\beta$ -actin was used as internal control to normalize gel loading. Bands were quantified by the aforementioned Scion Image beta 3b software.

### 11. Statistical analyses

Data from the control or drug-treatment groups were expressed as mean  $\pm$  SD and analyzed using one-way analysis of variance followed by Dennett's *post hoc* test in GraphPad Prism 4 (GraphPad Software Incorporation, San Diego, CA, USA). *p*-values <0.05 were considered significant.

## III. Results

### 1. Effect of GCBT on the cell viability of RAW 264.7 cells

The MTT assay was used to assess the cytotoxicity of GCBT on RAW264.7 cells treated for 4 hrs at a concentration of 1, 2.5, 5, 7.5, and 10 mg/mL. GCBT in the range of 1 to 10 mg/kg was not cytotoxic after 4 h (Fig. 1).

### 2. Effects of GCBT on the production and gene expression of proinflammatory cytokines in LPS-stimulated RAW264.7 cells

We examined whether GCBT suppressed the production and mRNA expression of the proinflammatory

cytokines TNF $\alpha$ , IL-1 $\beta$ , IL-6, GM-CSF, and INF $\gamma$  in LPS-stimulated RAW264.7 cells. Compared to the basal production levels of TNF $\alpha$ , IL-1 $\beta$ , IL-6, GM-CSF, and INF $\gamma$ , the production levels of these cytokines in LPS-stimulated RAW264.7 cells markedly increased. GCBT (2, 4, and 8 mg/mL) suppressed the production levels of TNF $\alpha$ , IL-1 $\beta$ , and IL-6 in a dose-dependent manner, and the production levels of GM-CSF and INF $\gamma$  in parallel (Fig. 2A). Compared to the basal mRNA levels of TNF $\alpha$ , IL-1 $\beta$ , IL-6, GM-CSF, and INF $\gamma$ , the mRNA levels of these cytokines in LPS-stimulated RAW264.7 cells were markedly increased. GCBT (2, 4, and 8 mg/mL) suppressed the mRNA levels of TNF $\alpha$ , IL-1 $\beta$ , IL-6, GM-CSF, and INF $\gamma$  on RAW264.7 cells in a dose-dependent manner (Fig. 2B).

### 3. Effects of GCBT on the production of Nitrite and PGE<sub>2</sub> and expression of iNOS and COX-2 in LPS-stimulated RAW264.7 cells

LPS stimulation typically induces inflammatory responses, such as iNOS/NO biosynthesis, in macrophages. Thus, we measured whether GCBT suppresses the production of nitrite by Griess reaction, iNOS protein levels by Western blot analysis, and iNOS mRNA levels by RT-PCR. Compared to the basal levels of nitrite and protein and mRNA of iNOS, the levels of those in LPS-stimulated RAW264.7 cells were markedly increased. GCBT (2, 4, and 8 mg/mL) reduced induction of those nitrite and iNOS protein and mRNA by LPS stimulation in a dose dependent manner (Fig. 3A). In inflammatory processes, excessive PGE<sub>2</sub> has a critical causa-

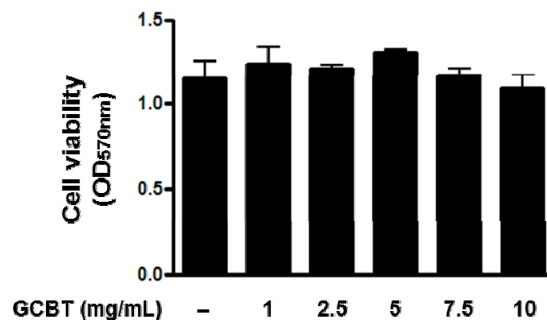


Fig. 1. Effect of GCBT on the cell viability of RAW264.7 cells

Cell viability was evaluated using a colorimetric assay based on MTT assay. Cells were preincubated with the diverse concentration of GCBT for 1 hr. The results are displayed in the absorbance at 570 nm. Results are presented as the mean  $\pm$  SD (n=3) for three independent experiments.

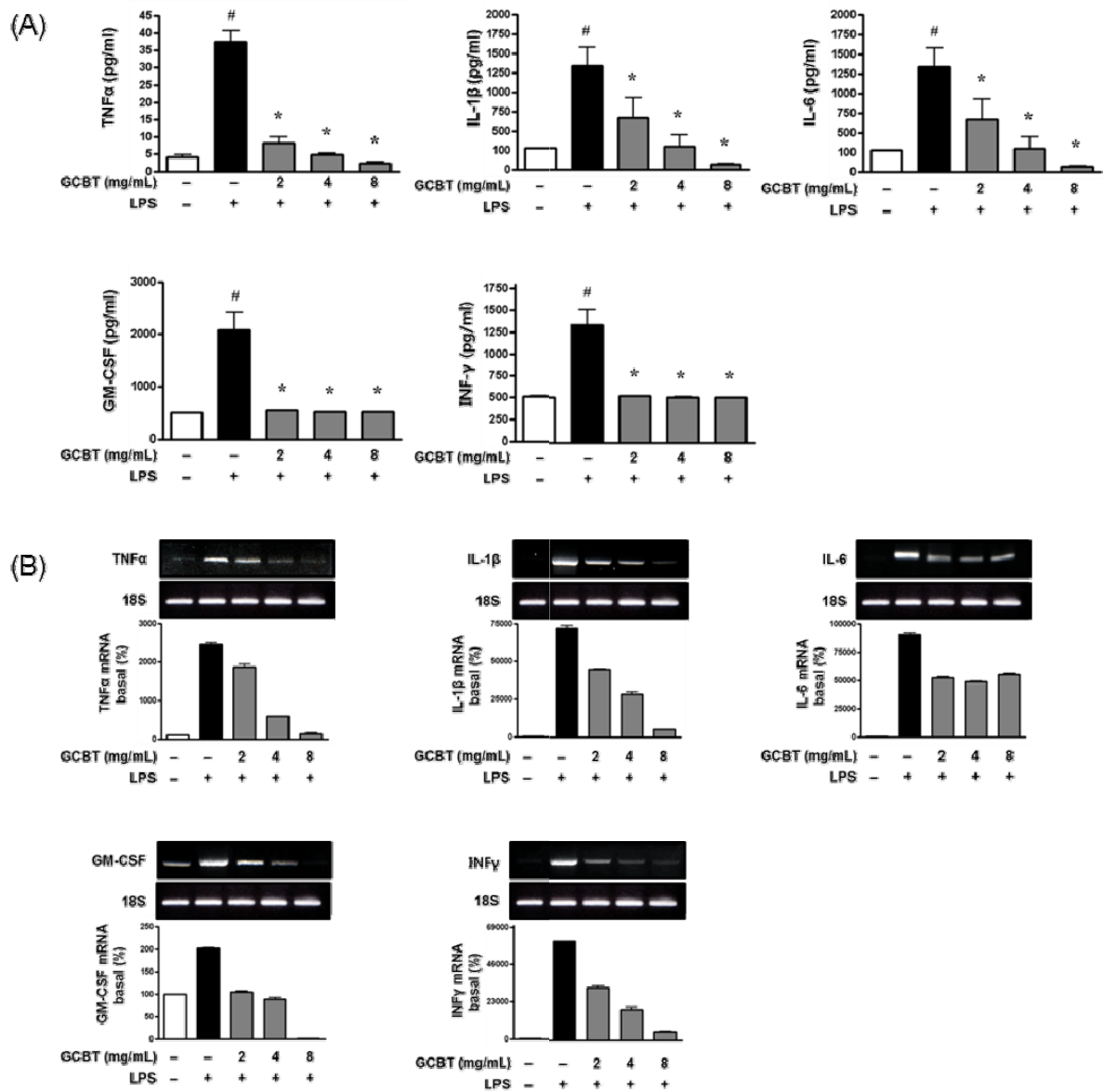


Fig. 2. Effects of GCBT on the production and gene expression of proinflammatory cytokines in LPS-stimulated RAW264.7 cells

(A) The concentration of proinflammatory cytokines was measured from cell supernatant using ELISA at 450 nm. Results represent as the mean±SD. # p<0.05 vs. vehicle group, \*p<0.05 vs. stimulated group (B) The expression of proinflammatory cytokines was evaluated by RT-PCR. 18S was used as an internal control.

tive role in many human diseases, including rheumatoid arthritis, asthma, and atherosclerosis. COX-2 is involved in the synthesis of prostaglandins. Thus, we measured whether GCBT suppresses the production of PGE<sub>2</sub> by ELISA, COX-2 mRNA levels by RT-PCR and COX-2 protein levels by Western blot analysis. Compared to the basal levels of PGE<sub>2</sub>, COX-2 protein, and COX-2 mRNA, the levels of those in LPS-stimulated RAW 264.7 cells were markedly increased. GCBT (2, 4, and

8 mg/mL) reduced induction of those enzyme genes by LPS stimulation in a dose-dependent manner (Fig. 3B).

#### 4. Effects of GCBT on LPS-stimulated ROS production in the RAW264.7 cells

ROS are generated under inflammation and injury, and ROS can cause cellular injury and death at higher concentrations. As ROS are critical for LPS-stimulated inflammation, we investigated the effects of GCBT on LPS-

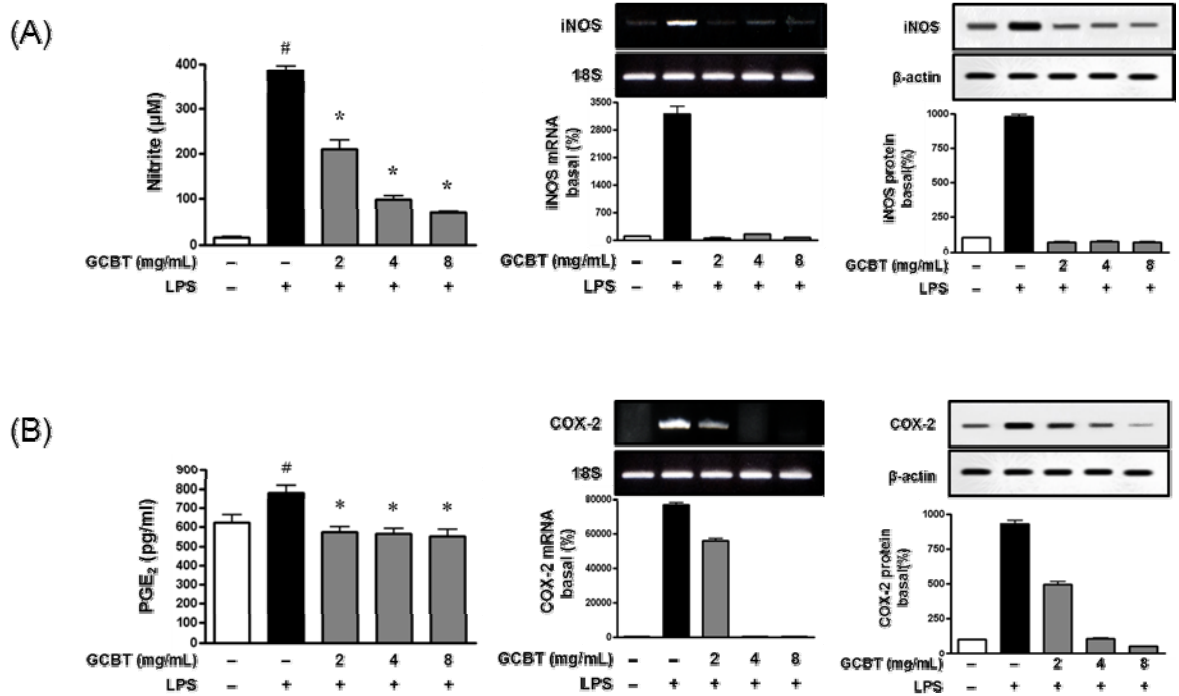


Fig. 3. Effects of GCBT on the production of nitrite and PGE<sub>2</sub>, and expression of iNOS and COX-2 in LPS-stimulated RAW264.7 cells

(A) Nitrite accumulation was measured colorimetrically by the Griess reaction. The absorbance was determined by an ELISA reader at 540 nm and calibrated using a sodium nitrite standard. (B) PGE<sub>2</sub> concentration was measured from cell supernatant using ELISA at 405 nm. Results represent as the mean ± SD. # p<0.05 vs vehicle group, \*p<0.05 vs stimulated group. The expression of gene and protein of iNOS and COX-2 was evaluated by RT-PCR and Western blotting. 18S and β-actin were used as an internal control.

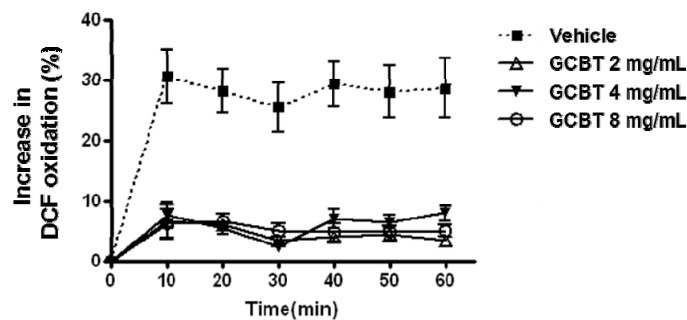


Fig. 4. Effects of GCBT on LPS-stimulated ROS production in the RAW264.7 cells

LPS-stimulated RAW264.7 cells were pre-incubated with 10 µM of H<sub>2</sub>DCF-DA for 30 min, washed twice with PBS, and treated with GCBT for 30 min. H<sub>2</sub>DCF-DA-loaded cells were stimulated with LPS for 1 hr, and ROS-mediated DCF oxidation was measured with excitation at 490 nm and emission at 530 nm with a fluorometer. The data are expressed as the percent increase in DCF oxidation above the vehicle group. \* p<0.05 vs vehicle group

stimulated ROS generation. GCBT (2, 4, and 8 mg/mL) markedly reduced LPS-stimulated upregulation of ROS in LPS-stimulated inflammatory responses. All concentrations of GCBT had a similar potent action (Fig. 4).

### 5. Effects of GCBT on the signal transduction in LPS-stimulated RAW264.7 cells

To clarify a molecular mechanism of the anti-inflammatory effect of GCBT, we detected the expression of the phosphorylation of MAPKs (ERK, JNK, and p38) and PI3K/Akt by Western blot analysis. LPS caused a rapid and significant increase in the phosphorylation of the three MAPKs and PI3K/Akt within 15 min. However, GCBT (2, 4, and 8 mg/mL) reduced phosphor-



Fig. 5. Effects of GCBT on the signal transduction in LPS-stimulated RAW264.7 cells

The phosphorylation of MAPK family (A), PI3K/Akt (B) and IκBα and expression of IκBα/nuclear NFκB (C) in LPS-stimulated Raw264.7 cells was evaluated by Western blotting. β-actin was used as an internal control.

ylation of the three MAPKs and PI3K/Akt in a dose-dependent manner (Fig. 5A). The effects of GCBT on LPS-stimulated IκBα proteolytic pathway and NFκB activation were examined by Western blot analysis for NFκB p65 translocation into the nucleus. NFκB p65 protein was detectable in the nucleus after LPS stimulation. However, GCBT completely blocked LPS-stimulated IκBα degradation and NFκB p65 nuclear translocation in a dose-dependent manner (Fig. 5B).

#### IV. Discussion

The present study was undertaken to identify the anti-inflammatory effect and anti-oxidant activities of GCBT on LPS-stimulated RAW264.7 cells. Inflammation is the result of host response to pathogenic challenge or tissue injuries. This process involves activated macrophages, such as RAW264.7 cells<sup>14</sup>.

Proinflammatory cytokines play key roles in the patho-



genesis of JRA. TNF- $\alpha$  was first described as a substance that destroys oncocytes. But it also has diverse effects on several cells including leukocytes and fibroblasts. Along with IL-1, TNF- $\alpha$  has a major role in destroying articular cartilage by boosting the expression of a breakdown enzyme for collagen fibers and protein and suppressing the formation of proteoglycan in fibroblasts or cartilage cells<sup>15</sup>. IL-1 $\beta$  is a carrier that activates chemokines, cytokines, and many other substances, such as synovial cells, endotheliocytes, lymphocytes, and macrophagocytes, which produces inflammation<sup>16,17</sup>. TNF $\alpha$  and IL-1 produced by activated monocytes, macrophages, and synovial fibroblasts likely have primary roles in the pathogenesis of JRA. These cytokines are detected in synovial fluids or tissues in a majority of JRA patients<sup>18,19</sup>, and stimulate mesenchymal cells, such as synovial fibroblasts, osteoclasts, and chondrocytes, to release tissue-destroying matrix metalloproteinases<sup>20</sup>. TNF $\alpha$  and IL-1 also inhibit synovial fibroblasts from producing tissue inhibitors of metalloproteinases. Collectively, these dual actions lead to joint damage<sup>14</sup>.

IL-1 has a prominent role in systemic onset disease. Treatment with IL-1 receptor antagonist reduces the clinical and laboratory features of disease activity in patients with systemic onset disease who show resistance to anti-TNF- $\alpha$  treatment<sup>21</sup>. IL-6 stimulated by TNF- $\alpha$  and IL-1 is a multifunction cytokine that has a wide range of biological activities in various target cells and regulates immune responses, acute phase reactions, hematopoiesis, and bone metabolism<sup>22</sup>. Circulating levels of IL-6 are markedly elevated in patients with JRA, and are associated with laboratory and clinical variables of disease activity<sup>10,23</sup>. Also, the circulating concentration of IL-6 is noticeably increased in patients with systemic onset disease and correlates with the extent of joint involvement<sup>7,24</sup>. In addition, IL-6 concentration is significantly higher in the synovial fluid of patients with systemic onset disease than in patients with other JRA subtypes<sup>25</sup>.

In the present study, GCBT significantly suppressed mRNA levels and the production levels of IL-1 $\beta$ , IL-6, and TNF- $\alpha$ , GM-CSF, and INF- $\gamma$  on LPS-stimulated RAW 264.7 cells in a dose-dependent manner (Fig. 2). NO, a highly reactive nitrogen radical, is produced by

iNOS. It has been implicated in multiple biological processes, and is an essential mediator of the host innate immune and inflammatory response to a variety of pathogens<sup>25</sup>. Excessive NO produced by iNOS mediates acute and chronic inflammation. So, the level of production of NO may reflect the degree of inflammation. Down-modulation of iNOS expression or suppression of NO has the potential to become a new pharmacological strategy for the treatment of the inflammatory-related diseases<sup>26,27</sup>. In inflammatory processes, COX-2 is expressed in many cells including fibroblasts and macrophages. COX-2 is considered to play a major role in the inflammatory process by catalyzing the production of PGE<sub>2</sub> that contributes to the pain and swelling of inflammation as an inflammatory mediator<sup>28-30</sup>. In RAW264.7 cells, LPS stimulus can induce iNOS and COX-2 transcription and translation, followed by NO and PGE<sub>2</sub> production<sup>31</sup>. Presently, GCBT reduced nitrite and PGE<sub>2</sub> production along with the protein levels of iNOS and COX-2 by suppressing iNOS and COX-2 gene expression in LPS-stimulated RAW264.7 cells (Fig. 3).

ROS refers not only to oxygen radicals, but also to non-radical derivatives of O<sub>2</sub><sup>32</sup>.

When ROS production is higher than the detoxification capacity of the cell, excessively generated ROS extensively damages DNA, proteins, and lipids, and mediates proinflammatory and carcinogenic events<sup>33</sup>. Also, ROS is involved in inflammatory gene expression through redox-based activation of the NF $\kappa$ B and COX-2 signaling pathways<sup>34</sup>. In the present study, GCBT markedly reduced LPS-induced upregulation of ROS in LPS-induced inflammatory responses (Fig. 4).

MAPK signaling pathways play a critical role in the regulation of inflammatory response and coordinate the induction of many genes encoding inflammatory mediators<sup>35</sup>. ERK, p38, and JNK have especially been implicated in the signal transduction pathways responsible for increased TNF- $\alpha$ , IL-1 $\beta$ , IL-6, iNOS, and COX-2 gene expression<sup>36-39</sup>. In this study, GCBT reduced phosphorylation and activation of the three MAPKs, which are crucial mediators in the regulation of inflammatory response, in a dose-dependent manner in LPS-stimulated RAW264.7 cells (Fig. 5A).

NF $\kappa$ B is an essential and ubiquitous transcription factor for the expression of many inflammation-related genes, including TNF- $\alpha$ , IL-1 $\beta$ , IL-6, iNOS, and COX-2<sup>40</sup>. Activation of the NF $\kappa$ B pathway is complex. It requires activation of PI3K/Akt upstream of I $\kappa$ B $\alpha$  degradation. NF $\kappa$ B activation pathway follows the sequence: TLR4 / IKK / I $\kappa$ B $\alpha$  / NF $\kappa$ B. Activation of the IKK complex results in phosphorylation and degradation of I $\kappa$ B $\alpha$ , permitting the nuclear translocation of the transcription factor, NF $\kappa$ B. This results in the expression of proinflammatory molecules<sup>41</sup>.

In the present study, LPS caused a rapid and significant increase in the phosphorylation of PI3K/Akt in RAW264.7 cells. However, GCBT reduced phosphorylation of PI3K/Akt in a dose-dependent manner. So, GCBT completely blocked the LPS-induced I $\kappa$ B $\alpha$  degradation, thereby inhibiting activation and translocation of NF $\kappa$ B (Fig. 5B and C).

In conclusion, GCBT significantly inhibited the release of proinflammatory cytokines (TNF $\alpha$ , IL-1 $\beta$ , IL-6, GM-CSF, and INF $\gamma$ ) and inflammatory mediators, together with their cognate mRNAs in a dose-dependent manner and had an anti-oxidative property. These effects were due to inhibition of LPS-induced phosphorylation of three MAPKs, PI3K/Akt, and I $\kappa$ B $\alpha$ , as well as nuclear translocation of NF $\kappa$ B. Therefore, GCBT might be a potential candidate anti-inflammatory drug for JRA.

## References

- Kim DS. Juvenile rheumatoid arthritis. *Korean J Pediatr.* 2007;50(12):1173.
- Phelan JD, Thompson SD. Genomic progress in pediatric arthritis: recent work and future goals. *Curr Opin Rheumatol.* 2006;18(5):482-9.
- Førre O, Smerdel A. Genetic epidemiology of juvenile idiopathic arthritis. *Scand J Rheumatol.* 2002;31(3):123-8.
- Murray K, Thompson S, Glass D. Pathogenesis of juvenile chronic arthritis: genetic and environmental factors. *Arch Dis Child.* 1997;77(6):530-4.
- Brewer EJ Jr, Bass J, Baum J, Cassidy JT, Fink C, Jacobs J, Hanson V, Levinson JE, Schaller J, Stillman JS. Current proposed revision of JRA criteria. JRA Criteria Subcommittee of the Diagnostic and Therapeutic Criteria Committee of the American Rheumatism Section of The Arthritis Foundation. *Arthritis Rheum.* 1997;20(2):195-9.
- De Benedetti F, Martini A. Is systemic juvenile rheumatoid arthritis an interleukin 6 mediated disease? *J Rheumatol.* 1998;25(2):203-7.
- De Benedetti F, Massa M, Pignatti P, Albani S, Novick D, Martini A. Serum soluble interleukin 6 (IL-6) receptor and IL-6/soluble IL-6 receptor complex in systemic juvenile rheumatoid arthritis. *J Clin Invest.* 1994;93(5):2114-9.
- Woo P. The cytokine network in juvenile chronic arthritis. *Rheum Dis Clin North Am.* 1997;23(3):491-8.
- Morimoto C, Reinherz EL, Borel Y, Mantzouranis E, Steinberg AD, Schlossman SF. Autoantibody to an immunoregulatory inducer population in patients with juvenile rheumatoid arthritis. *J Clin Invest.* 1981;67(3):753-61.
- Mangge H, Kenzian H, Gallistl S, Neuwirth G, Liebmann P, Kaulfersch W, Beaufort F, Muntean W, Schauenstein K. Serum cytokines in juvenile rheumatoid arthritis. Correlation with conventional inflammation parameters and clinical subtypes. *Arthritis Rheum.* 1995;38(2):211-20.
- Hahn YS, Kim JG. Pathogenesis and clinical manifestations of juvenile rheumatoid arthritis. *Korean J Pediatr.* 2010;53(11):921-30.
- Choi J, Lee C. A clinical study of juvenile rheumatoid arthritis. *J Oriental Rehab Med.* 1998;18(2):306-17.
- The Korean Academy of Oriental Rehabilitation Medicine ed. *Oriental rehabilitation medicine.* Seoul: Koonja. 2005:78-99.
- Kaplanski G, Marin V, Montero-Julian F, Mantovani A, Farnarier C. IL-6: a regulator of the transition from neutrophil to monocyte recruitment during inflammation. *Trends Immunol.* 2003;24(1):25-9.
- Williams RO, Feldmann M, Maini RN. Anti-tumor necrosis factor ameliorates joint disease in murine collagen-induced arthritis. *Proc Natl Acad Sci USA.* 1992;89(20):9784-8.

16. Feldmann M, Brennan FM, Maini RN. Rheumatoid Arthritis. *Cell*. 1996;85:307-10.
17. Hom JT, Bendele AM, Carlson DG. In vivo administration with IL-1 accelerates the development of collagen-induced arthritis in mice. *J Immunol*. 1988;141(3): 834-41.
18. Grom AA, Murray KJ, Luyrink L, Emery H, Passo MH, Glass DN, Bowlin T, Edwards AC 3<sup>rd</sup>. Patterns of expression of tumor necrosis factor alpha, tumor necrosis factor beta, and their receptors in synovia of patients with juvenile rheumatoid arthritis and juvenile spondylarthropathy. *Arthritis Rheum*. 1996;39(10): 1703-10.
19. Kutukculer N, Caglayan S, Aydogdu F. Study of pro-inflammatory (TNF-alpha, IL-1alpha, IL-6) and T-cell-derived (IL-2, IL-4) cytokines in plasma and synovial fluid of patients with juvenile chronic arthritis: correlations with clinical and laboratory parameters. *Clin Rheumatol*. 1998;17(4):288-92.
20. Shingu M, Nagai Y, Isayama T, Naono T, Nobunaga M, Nagai Y. The effects of cytokines on metalloproteinase inhibitors (TIMP) and collagenase production by human chondrocytes and TIMP production by synovial cells and endothelial cells. *Clin Exp Immunol*. 1993;94(1):145-9.
21. Pascual V, Allantaz F, Arce E, Punaro M, Banchereau J. Role of interleukin-1 (IL-1) in the pathogenesis of systemic onset juvenile idiopathic arthritis and clinical response to IL-1 blockade. *J Exp Med* 2005;201(9):1479-86.
22. Nishimoto N, Kishimoto T. Interleukin 6: from bench to bedside. *Nat Clin Pract Rheumatol*. 2006;2(11):619-26.
23. Ou LS, See LC, Wu CJ, Kao CC, Lin YL, Huang JL. Association between serum inflammatory cytokines and disease activity in juvenile idiopathic arthritis. *Clin Rheumatol*. 2002;21(1):52-6.
24. De Benedetti F, Massa M, Robbioni P, Ravelli A, Burgio GR, Martini A. Correlation of serum interleukin-6 levels with joint involvement and thrombocytosis in systemic juvenile rheumatoid arthritis. *Arthritis Rheum*. 1991;34(9):1158-63.
25. De Benedetti F, Pignatti P, Gerloni V, Massa M, Sartirana P, Caporali R, Montecucco CM, Corti A, Fantini F, Martini A. Differences in synovial fluid cytokine levels between juvenile and adult rheumatoid arthritis. *J Rheumatol*. 1997;24(7):1403-9.
26. Wallace JL. Nitric oxide as a regulator of inflammatory processes. *Mem Inst Oswaldo Cruz*. 2005;100(1):5-9.
27. Tinker AC, Wallace AV. Selective inhibitors of inducible nitric oxide synthase: potential agents for the treatment of inflammatory diseases? *Curr Top Med Chem*. 2006;6(2):77-92.
28. Vane JR, Mitchell JA, Appleton I, Tomlinson A, Bishop-Bailey D, Croxtall J, Willoughby DA. Inducible isoforms of cyclooxygenase and nitric-oxide synthase in inflammation. *Proc Natl Acad Sci USA*. 1994;91(6):2046-50.
29. Hla T, Ristimäki A, Appleby S, Barriocanal JG. Cyclooxygenase gene expression in inflammation and angiogenesis. *Ann NY Acad Sci*. 1993;696:197-204.
30. Dubois RN, Abramson SB, Crofford L, Gupta RA, Simon LS, Putte LBAVD, Lipsky PE. Cyclooxygenase in biology and disease. *FASEB J*. 1998;12(12):1063-73.
31. Liang YC, Huang YT, Tsai SH, Lin-Shiau SY, Chen CF, Lin JK. Suppression of inducible cyclooxygenase and inducible nitric oxide synthase by apigenin and related flavonoids in mouse macrophages. *Carcinogenesis*. 1999;20(10):1945-52.
32. Floyd RA. Neuroinflammatory processes are important in neurodegenerative diseases: an hypothesis to explain the increased formation of reactive oxygen and nitrogen species as major factors involved in neurodegenerative disease development. *Free Radic Biol Med*. 1999;26(9-10): 1346-55.
33. Cesaratto L, Vascotto C, Calligaris S, Tell G. The importance of redox state in liver damage. *Ann Hepatol*. 2004;3(3):86-92.
34. Kabe Y, Ando K, Hirao S, Yoshida M, Handa H. Redox regulation of NF-kappaB activation: distinct redox regulation between the cytoplasm and the nucleus. *Antioxid Redox Signal*. 2005;7(3-4):395-403.
35. Zhang W, Liu HT. MAPK signal pathways in the regulation of cell proliferation in mammalian cells. *Cell Res*. 2002;12(1):9-18.
36. Silva JD, Pierrat B, Mary JL, Lesslauer W. Blockade of p38 mitogen-activated protein kinase pathway inhibits

- inducible nitric-oxide synthase expression in mouse astrocytes. *J Biol Chem.* 1997;272(45):28373-80.
37. Murphy GM, Yang L, Cordell B. Macrophage colony-stimulating factor augments  $\beta$ -amyloid-induced interleukin-1, interleukin-6, and nitric oxide production by microglial cells. *J Biol Chem.* 1998;273(33):20967-71.
38. Xu X, Malave A. p38 MAPK, but not p42/p44 MAPK mediated inducible nitric oxide synthase expression in C6 glioma cells. *Life Sci.* 2000;67(26):3221-30.
39. Fiebich BL, Lieb K, Engels S, Heinrich M. Inhibition of LPS-induced p42/44 MAP kinase activation and iNOS/NO synthesis by parthenolide in rat primary microglial cells. *J Neuroimmunol.* 2002;132(1):18-24.
40. Christman JW, Blackwell TS, Juurlink BH. Redox regulation of nuclear factor kappa B: therapeutic potential for attenuating inflammatory responses. *Brain Pathol Zurich Switz.* 2002;10(1):153-62.
41. Dauphinee SM, Karsan A. Lipopolysaccharide signaling in endothelial cells. *Lab Invest.* 2005;86(1):9-22.